

3D printed nanocomposites using polymer grafted graphene oxide prepared by multicomponent Passerini reaction

Guannan Wang, Raju Raju, Kiho Cho, Sandy Wong, B.Gangadhara Prusty and Martina H. Stenzel

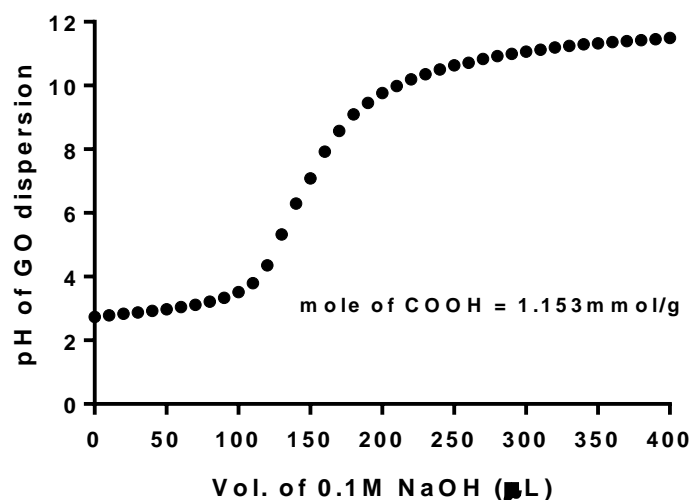
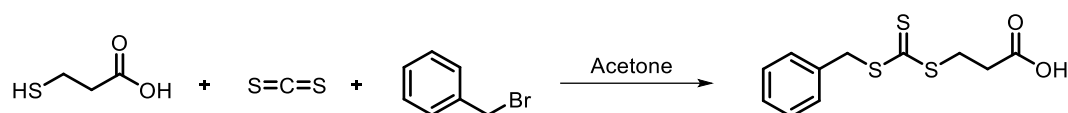


Figure S1. pH titration curve of unmodified GO dispersion by adding 0.1M NaOH solution. (mole of -COOH group = 1.153 mmol per gram of unmodified GO)

Synthesis of 3-(benzylsulfanylthiocarbonylsulfanyl) propionic acid (BSPA)



Scheme S1. Synthesis of 3-(benzylsulfanylthiocarbonylsulfanyl) propionic acid.

BSPA was prepared using a procedure reported earlier (**Scheme S1**).¹ To a 50 ml round-bottom flask, equipped with a magnetic stirring bar, tripotassium phosphate (K_3PO_4) (4.872 g, 22.95 mmol) and reagent-grade acetone (48.7 ml) were added. After adding K_3PO_4 , suspended in acetone, the mixture was stirred with 3-mercaptopropionic acid (2.436 g, 22.95 mmol) for 10 minutes. Then, carbon disulfide (CS_2) (4.1 ml 67.85 mmol) was added dropwise with stirring resulting in the formation of a yellow solution. After stirring for another 10 minutes, benzyl bromide (2.7 ml, 22.90 mmol) was added into the solution. The solution was stirred for 30 minutes afterward. The solvent was subsequently removed under reduced pressure and the residue was suspended in saturated brine solution (200 ml) and extracted with dichloromethane (DCM) (2×200 ml). The organic layer was kept and washed with brine solution (3×200 ml). Finally, the organic layer was dried by magnesium sulfate ($MgSO_4$) and filtered to remove

MgSO₄. Bright yellow BSPA crystals were obtained with 90% yield and 99 % purity after removing the solvent under reduced pressure. The monomer was characterized by ¹H NMR (Figure S3)

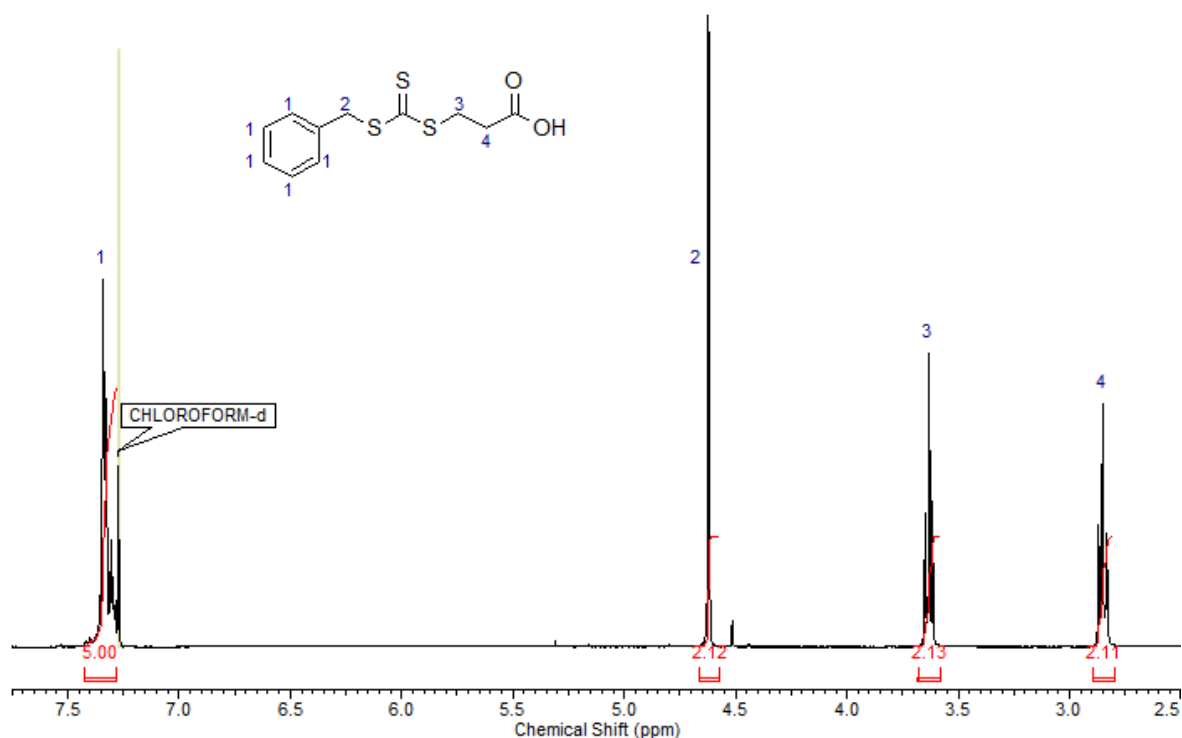
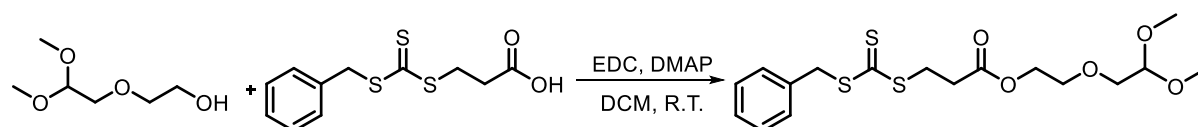


Figure S2. ¹H-NMR spectrum of BSPA in CDCl₃.

Synthesis of 2-(2,2-dimethoxy-ethoxy) ethyl 3-(benzylthiocarbothioylthio)propanoate (BSPA-acetal)



Scheme S2. Synthesis of 2-(2,2-dimethoxy-ethoxy) ethyl 3-(benzylthiocarbothioylthio) propanoate (BSPA-acetal).

RAFT-acetal RAFT agent was synthesized using a procedure developed in our group earlier (Scheme S2).² To a 250 ml round bottom flask equipped with a magnetic stirrer bar, BSPA (3.0 g, 11.00 mmol), 2-(2,2-dimethoxy-ethoxy)-ethanol (8.0 g, 53.27 mmol) and 60 mL of DCM were added and stirred until fully dissolved. The mixture was cooled with an ice bath and then 4-(dimethylamino)pyridine (DMAP) (1.38 g, 11.30 mmol) and *N*-(3-dimethylaminopropyl)-*N'*-ethylcarbodiimide hydrochloride (EDC·HCl) (5.6 g, 29.21 mmol) in DCM (40 ml) was added dropwise into the BSPA DCM solution. The solution was stirred for 2 hours at 0 °C, and further stirred for 40 hours at room temperature. Then, the solution was added into a saturated solution of brine (100 ml) and extracted with dichloromethane (DCM) (100 ml). The organic

layer was washed with brine solution (2×100 ml) and dried with magnesium sulfate (MgSO₄). The suspension was and filtered to remove MgSO₄. The solvent was removed under reduced pressure. After purification by flash chromatography using hexane/ethyl acetate = 50/50 v/v, the product was obtained as yellow liquid. The structure of the RAFT-acetal was confirmed by ¹H-NMR (**Figure S4**).

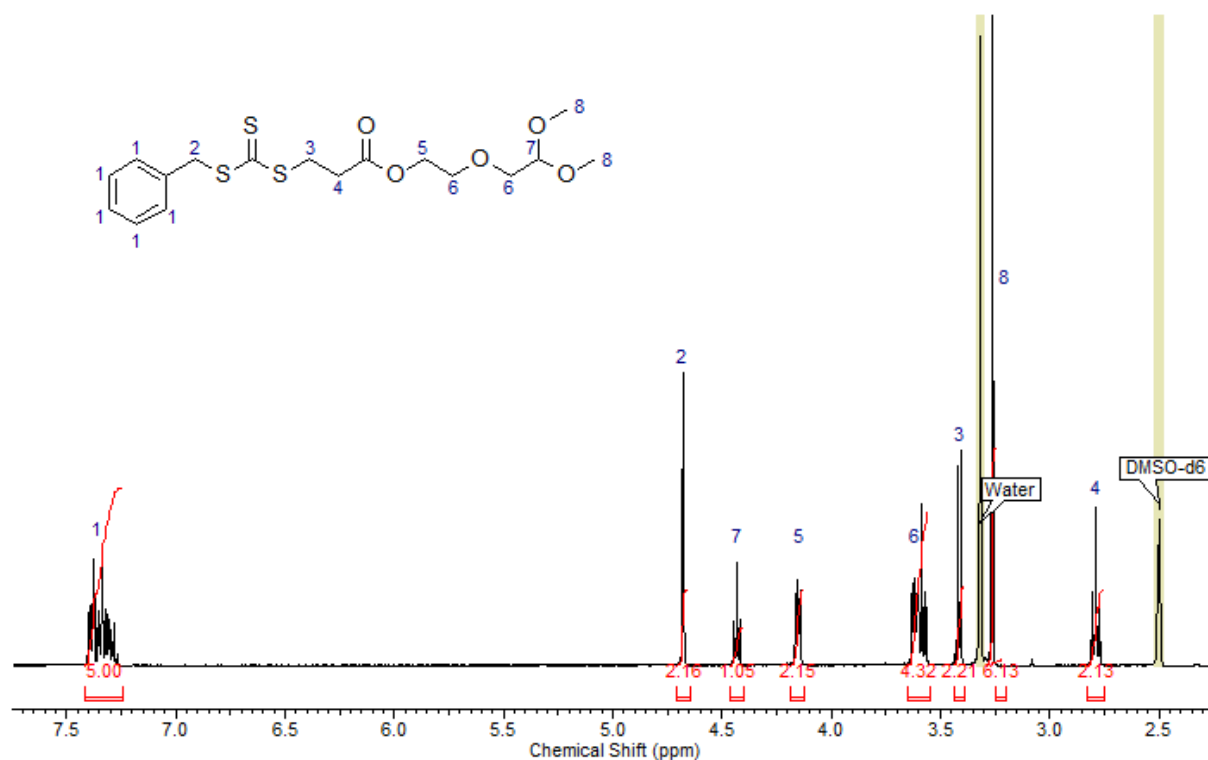
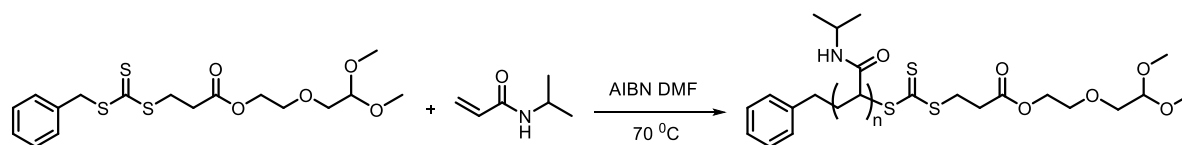


Figure S3. ¹H-NMR spectrum of 2-(2,2-dimethoxy-ethoxy) ethyl 3-(benzylthiocarbonothioylthio) propanoate (BSPA-acetal) in DMSO-d₆.

Synthesis of poly(N-isopropylacrylamide) with acetal ending group (PNIPAM-acetal) via Reversible Addition-Fragmentation Chain-Transfer (RAFT) polymerization



Scheme S3. Synthesis of PNIPAM-acetal

PNIPAM was polymerized using an earlier procedure.² PNIPAM of different molecular weights was synthesized by adjusting the molar ratios of monomers to BSPA-acetal (**Table S1**). For example, 1.00g (8.84mmol) *N*-isopropylacrylamide (NIPAM), 35.8mg (88.3μmol) BSPA-acetal and 1.45mg (8.83 μmol) AIBN were dissolved in DMF to yield a monomer concentration of 5.89 M. The solution was added into a 10ml round bottom flask equipped with

a magnetic stirrer bar. The round bottom flask was then sealed with a rubber septum and purged with nitrogen for 45 mins to remove oxygen from the system. The deoxygenated round bottom flask was then immersed into a 70°C oil bath and the mixture was stirred at 500 rpm. The polymerization was stopped after 2 hours by removing the rubber septum and placing the round bottom flask in an ice bath. The polymer was then obtained by dialysis in methanol for a day and then dialysis in milli-Q water for three days using 3500 MWCO dialysis membrane. The polydispersity of the synthesized polymer was determined by size exclusion chromatography (SEC) in DMF after freeze drying. The monomer conversion of NIPAM was determined by 400MHz $^1\text{H-NMR}$ in CDCl_3 .

Table S1. Experimental conditions for the preparation of PNIPAM with different chain lengths

Name	NIPAM	BSPA-acetal	AIBN	Molar ratio NIPAM:BSPA- acetal:AIBN	Reaction Time
PNIPAM ₈₀	1.0 g	35.8 mg	1.45 mg	100:1:0.1	120 mins
PNIPAM ₁₂₀	1.0 g	18 mg	0.72 mg	200:1:0.1	120 mins
PNIPAM ₂₂₈	1.0 g	9 mg	0.36 mg	400:1:0.1	120 mins

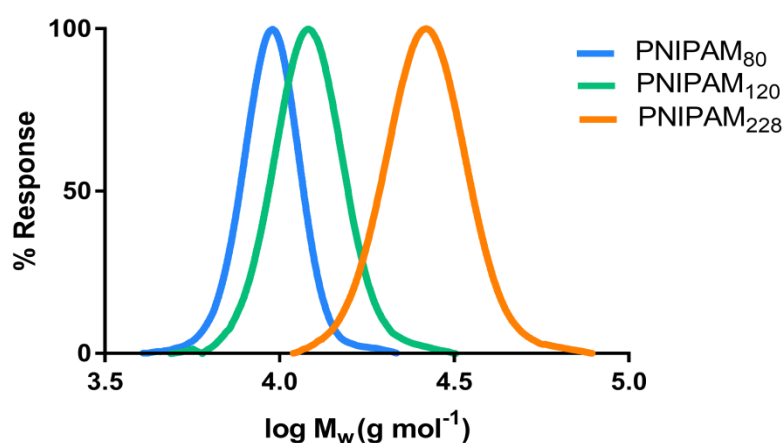
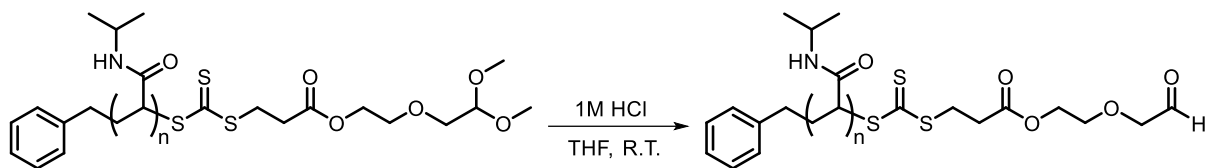


Figure S4. SEC traces of PNIPAMs with different chain lengths

Preparation of poly(N-isopropylacrylamide) with aldehyde ending group (PNIPAM-CHO)



Scheme S4. Preparation of PNIPAM-CHO from PNIPAM-acetal.

The aldehyde group was liberated by deprotecting the acetal in a mixture of THF and 1M HCl (**Scheme S4**). In a glass vial equipped with a magnetic stirrer bar, 2.5 ml 1M HCl was mixed with 3.0 ml THF. Around 200 mg polymer was added into the solvent mixture and stirred for 72 hours to ensure that all acetal ending groups were deprotected into aldehyde groups. The PNIPAM-CHO sample was obtained by dialysis against methanol for 2 times and against milli-Q water for another 2 times, followed by freeze drying.

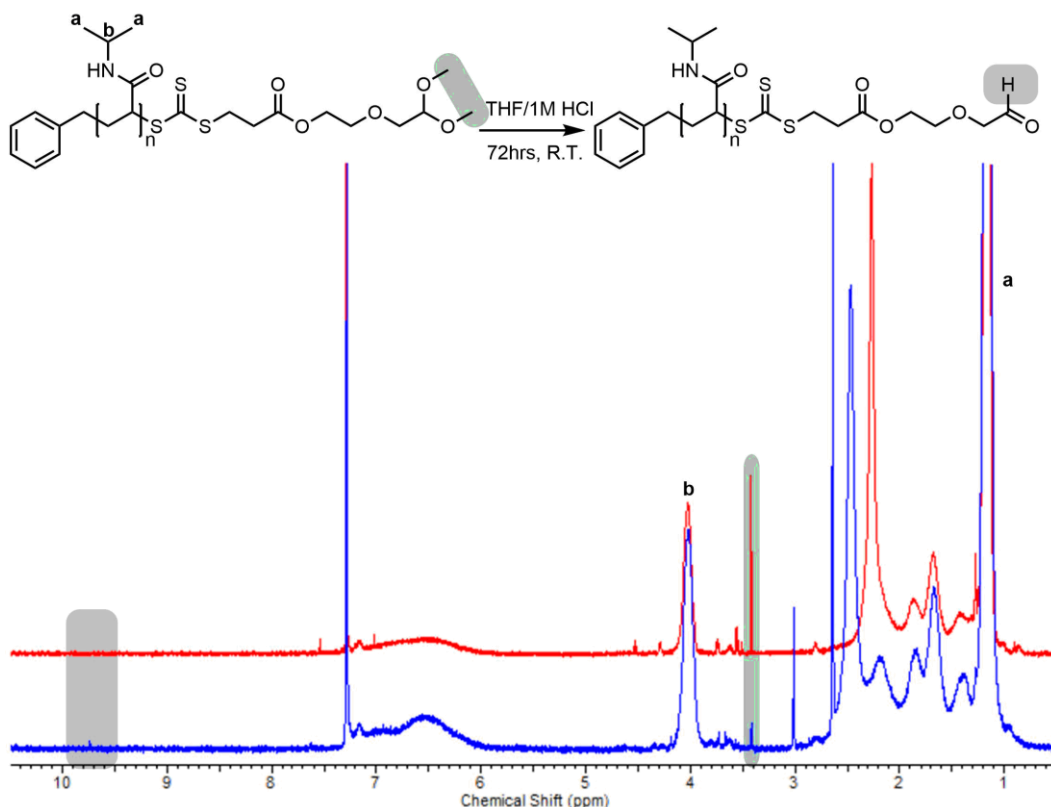


Figure S5. NMR spectra in CDCl_3 of PNIPAMs before (red) and after endgroup deprotection (blue)

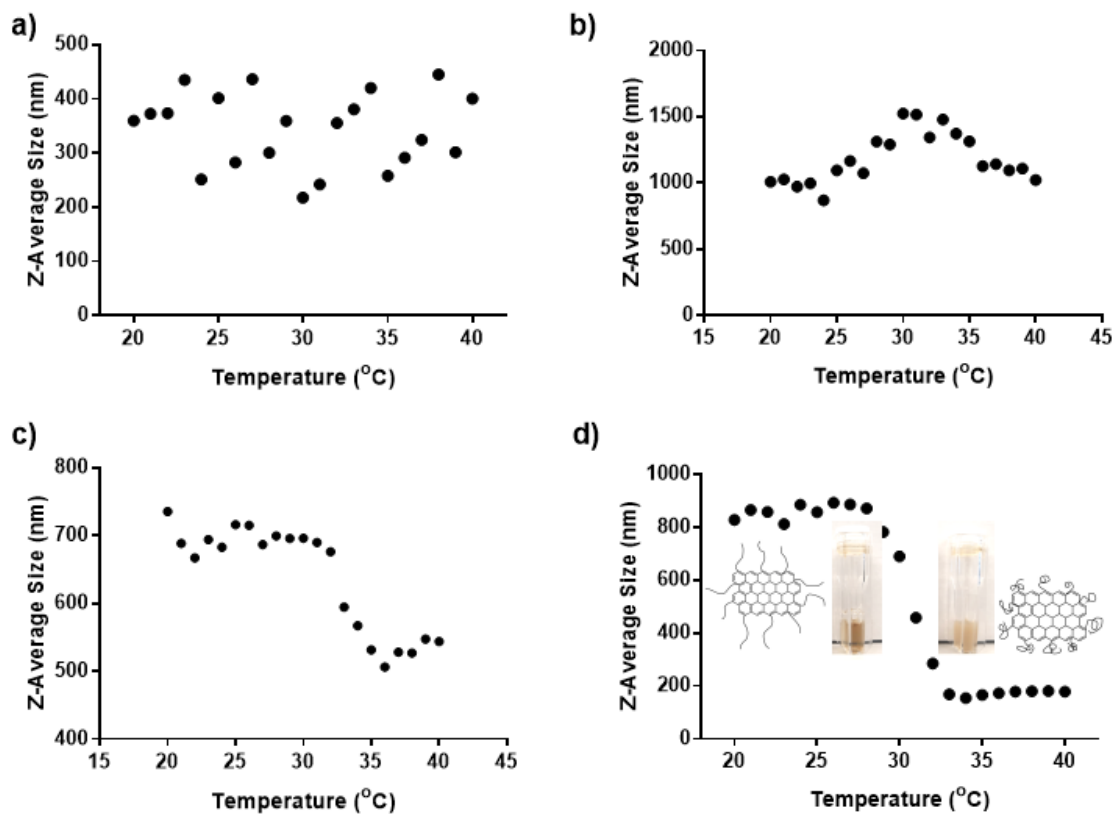


Figure S6. DLS z-average size measurements of a) 1.5mg/ml GO in milli-Q water; b) 1.5mg/ml GO-PNIPAM₈₀; c) 1.5mg/ml GO-PNIPAM₁₂₀; and d) 1.5mg/ml GO-PNIPAM₂₂₈ in milli-Q water at temperatures from 20.0°C to 40.0°C.

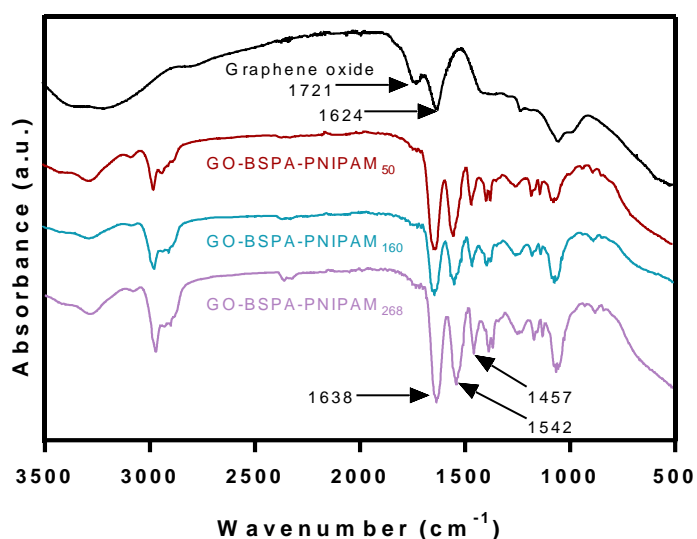


Figure S7. FT-IR spectra of pure GO (black), GO-BSPA-PNIPAM₅₀ (brown), GO-BSPA-PNIPAM₁₆₀ (blue) and GO-BSPA-PNIPAM₂₆₈ (purple).

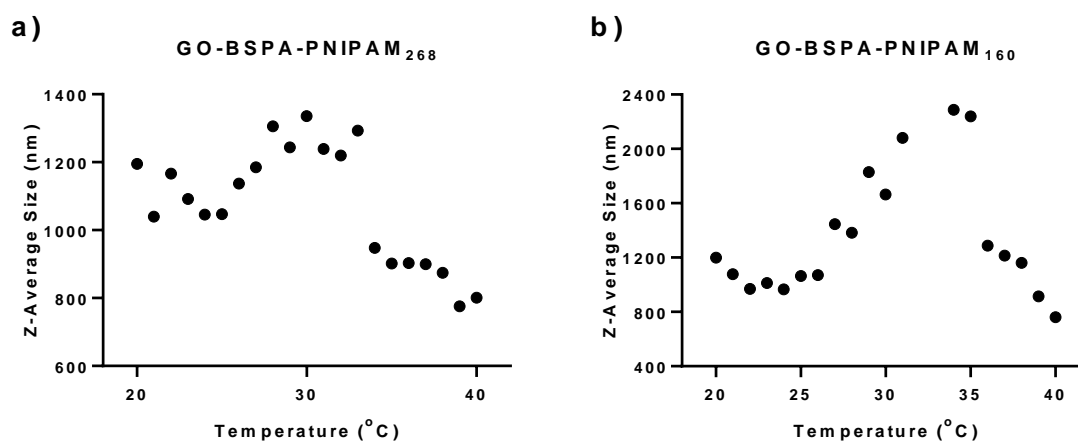


Figure S8. Changes in hydrodynamic diameter in the temperature range of 20.0°C to 40.0°C of GO-BSPA-PNIPAM₂₆₈ and GO-BSPA-PNIPAM₁₆₀ in milli-Q water monitored by DLS.

Table S2. GO reinforcement application from previous works

Matrix materials	Best mechanical property the composites can reach	Amount of GO in sample with best mechanical property	Ref.
Bis-GMA/TEGDMA (70/30, w/w)	Flexural modulus increased up to 72% than pure resin	0.1 wt% GO-BSPA-PNIPAM ₂₆₈	This work
Poly (l-lactic acid) (PLLA)	Young's modulus increased 59.6% than pure PLLA	2.0 wt% GO	3
Polycaprolactone (PCL)	Young's modulus increased 109.5% than pure PCL	2.0 wt% GO	
Polystyrene (PS)	Young's modulus increased 95.6% than pure PS	2.0 wt% GO	
High-density polyethylene (HDPE)/ Maleic Anhydride-Grafted-polyethylene (MAPE) (90/10, wt/wt%)	Young's modulus increased 34.8% than pure HDPE/MAPE mixture	0.3 wt% GO	4
Poly(methyl methacrylate) (PMMA)	Young's modulus increased 16.6% than pure PMMA	1.0wt% PMMA grafted GO	
Cement	Elastic modulus increased 6.3% than pure cement	0.05wt% GO	5

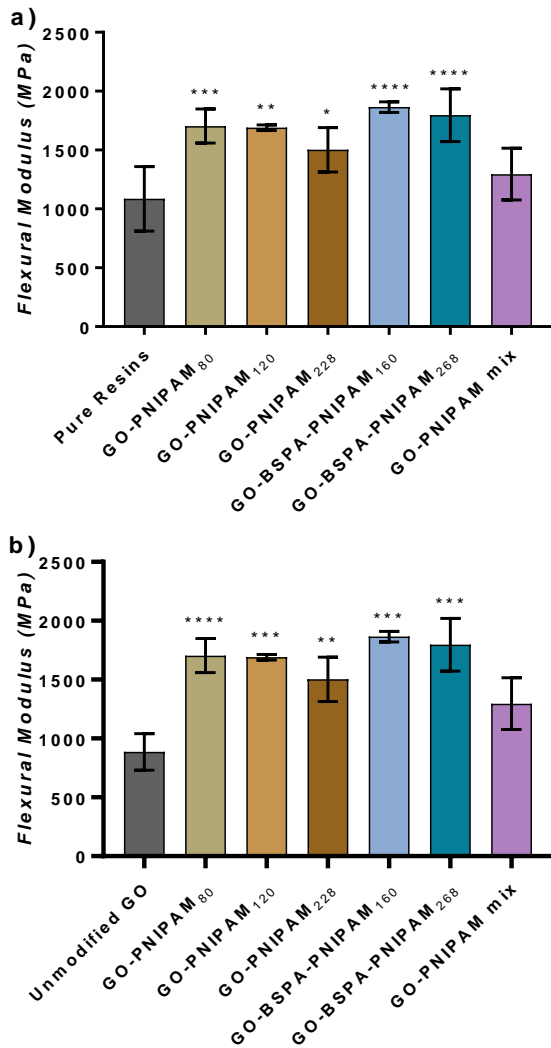


Figure S9. Statistical analysis by one-way ANOVA method of Bis-GMA/TEGDMA (70/30) resin adding 0.10 wt% modified GOs with a) pure resin as the control group and b) resin with 0.10 wt% unmodified GO as the control group. $p < 0.05$ is marked with “*” indicating statistically low significant difference, $p < 0.01$ is marked with “**” indicating statistically medium significant difference, $p < 0.001$ is marked with “***” indicating statistically high significant difference, while $p < 0.0001$ is marked with “****” indicating statistically very high significant difference.

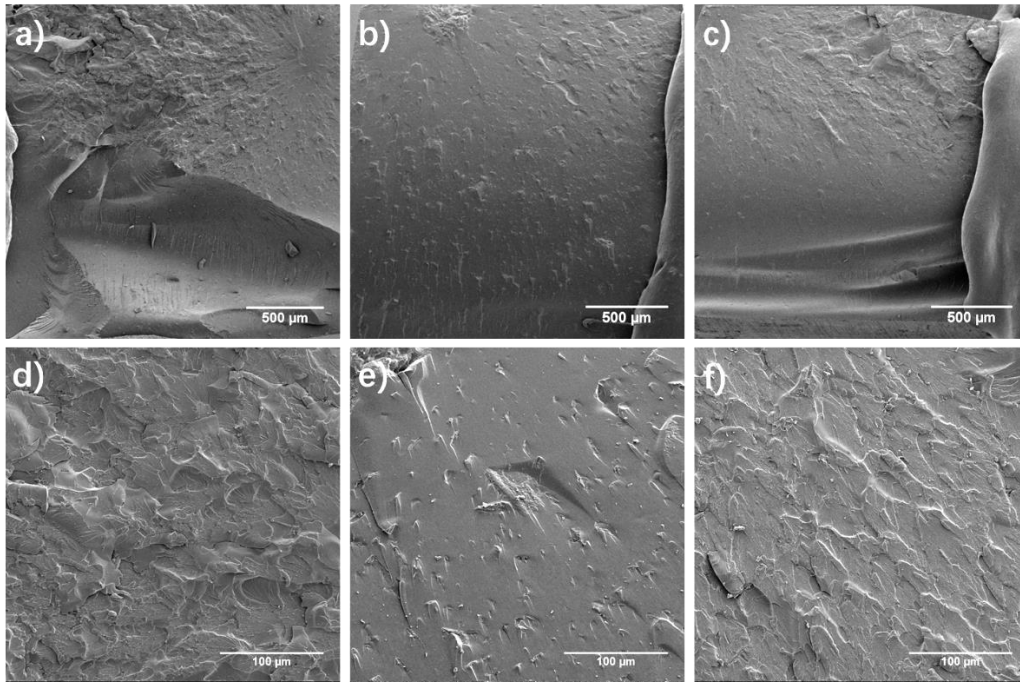


Figure S10. SEM images of the fracture surface of 3D printed Bis-GMA/TEGDMA (70/30) copolymer with 0.10 wt% a) & d) GO-PNIPAM₈₀; b) & e) GO-PNIPAM₁₂₀; c) & f) GO-PNIPAM₂₂₈

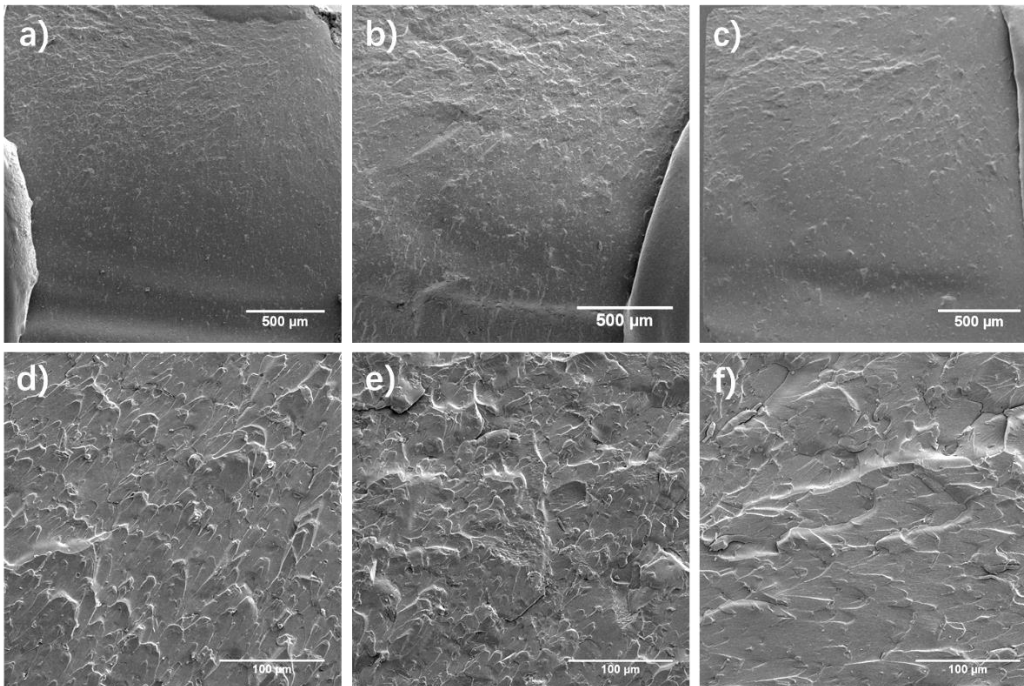


Figure S11. SEM images of the fracture surface of 3D printed Bis-GMA/TEGDMA (70/30) copolymer with 0.50 wt% a) & d) GO-PNIPAM₈₀; b) & e) GO-PNIPAM₁₂₀; c) & f) GO-PNIPAM₂₂₈

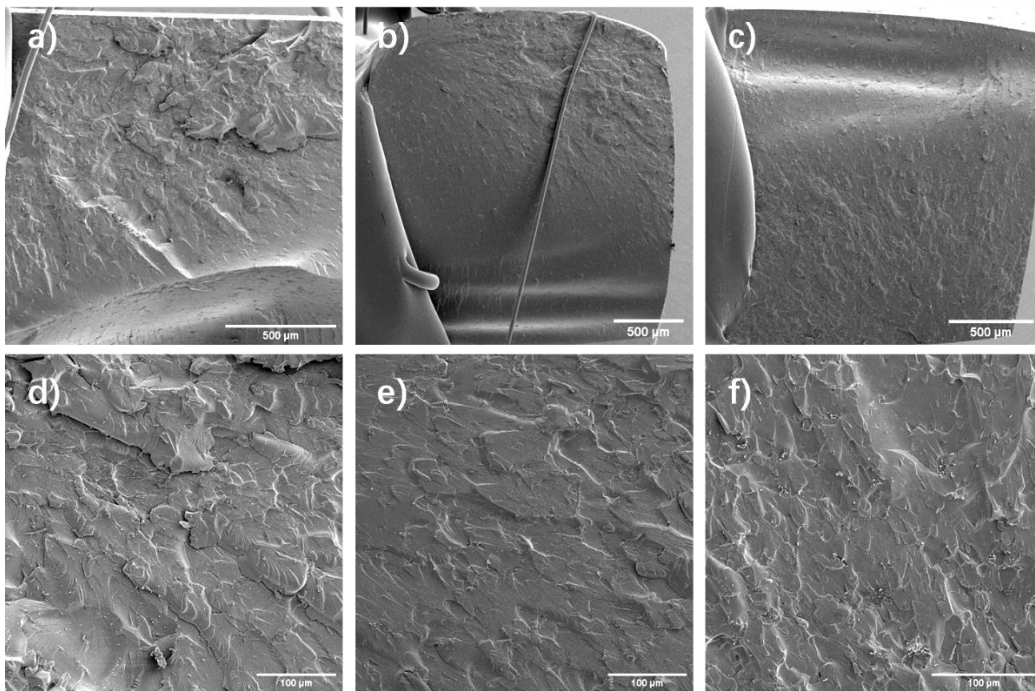


Figure S12. SEM images of the fracture surface of 3D printed Bis-GMA/TEGDMA (70/30) copolymer with a) & d) 0.05 wt%; b) & e) 0.10 wt% and c) & f) 0.50 wt% GO-BSPA-PNIPAM₁₆₀

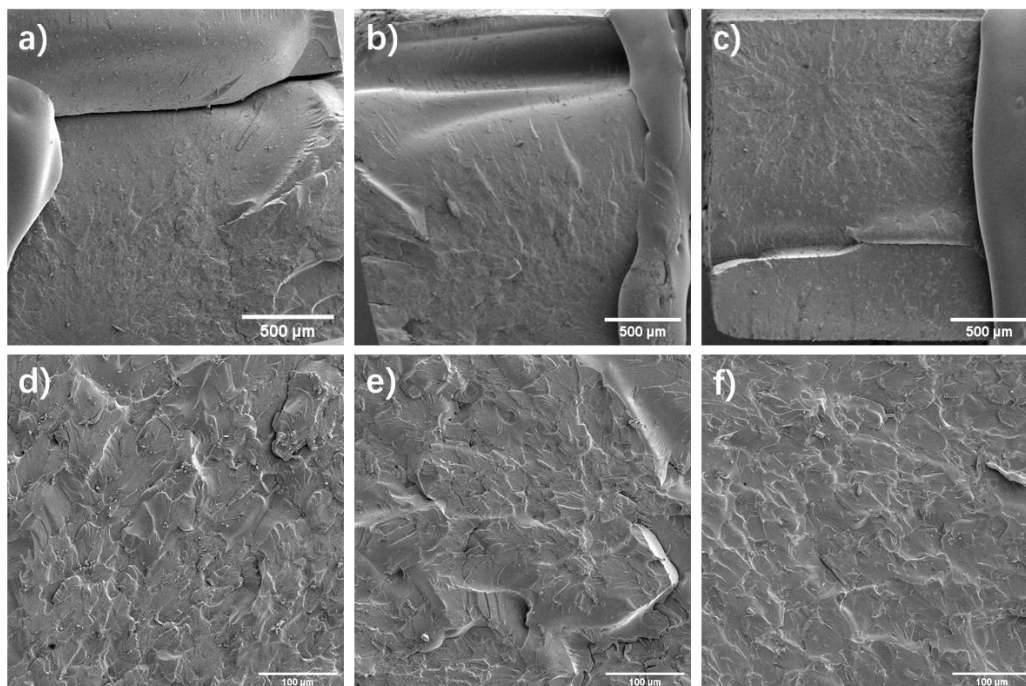


Figure S13. SEM images of the fracture surface of 3D printed Bis-GMA/TEGDMA (70/30) copolymer with a) & d) 0.05 wt%; b) & e) 0.10 wt% and c) & f) 0.50 wt% GO-BSPA-PNIPAM₂₆₈

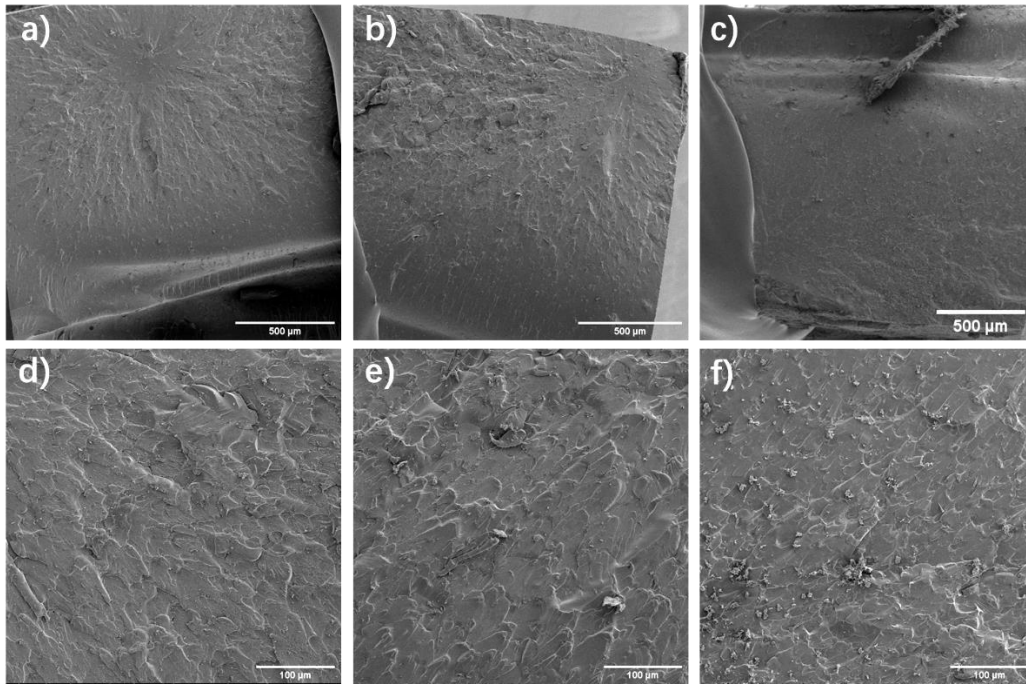


Figure S14. SEM images of the fracture surface of 3D printed Bis-GMA/TEGDMA (70/30) copolymer with a) & d) 0.05 wt%; b) & e) 0.10 wt% and c) & f) 0.50 wt% GO-PNIPAM_{mix}

References

1. J. Skey and R. K. O'Reilly, *Chem. Commun.*, 2008, 4183-4185.
2. Y. Y. Khine, S. Ganda and M. H. Stenzel, *ACS Macro Lett.*, 2018, **7**, 412-418.
3. C. Wan and B. Chen, *Journal of Materials Chemistry*, 2012, **22**, 3637-3646.
4. G. Gonçalves, P. A. Marques, A. Barros-Timmons, I. Bdkin, M. K. Singh, N. Emami and J. Grácio, *J. Mater. Chem.*, 2010, **20**, 9927-9934.
5. S. Chuah, Z. Pan, J. G. Sanjayan, C. M. Wang and W. H. Duan, *Construction and Building Materials*, 2014, **73**, 113-124.